KINETICS OF CORROSION OF HIGH ALUMINA REFRACTORIES BY MOLTEN OXIDES WITH TIME-RESOLVED HIGH-TEMPERATURE X-RAY DIFFRACTION

Emmanuel de Bilbao[1], Mathieu Dombrowski[1], Henry Pillière[2], Jacques Poirier[1]

[1] CNRS, CEMHTI UPR3079, Univ. Orléans, Orléans, France
[2] ThermoFisher Scientific, Artenay, France

ABSTRACT

This work aimed at quantifying the time-dependent corrosion of high alumina refractories by Al_2O_3-CaO-SiO_2 slag. The main objectives were i) to determine corrosion kinetics based on time-resolved X-ray diffraction at high temperature combined with Rietveld quantification and ii) to propose a reaction model based on dissolution / precipitation / diffusion mechanism. The tests were performed at temperature ranging from 1500 °C up to 1600 °C. The results show that the corrosion process is very fast and involves an indirect dissolution mechanism.

INTRODUCTION

In steel making, high alumina refractory bricks and alumina-magnesia in situ spinel castables are used successfully in the steel ladles, particularly in the wall, the bottom and the impact pad ladles. In the case of secondary metallurgy, the slag is primarily composed of lime and alumina and may contain also other slag oxides (FeO_x, MnO, MgO, SiO_2). During corrosion, the slag penetrates the porous matrix and reacts with the forming spinel solid solutions (fig. 1-a) or the mullite phase (bauxite or andalusite bricks). The impoverished slag reacts then with the high alumina aggregates to produce lime-aluminates layers limiting the dissolution of the aggregates (fig. 1-b). Slag penetration coupled with dissolution/precipitation mechanism leads to chemical spalling with varying degrees. These most important phenomena control the service life of refractories. The corrosion rate depends then on the kinetics of penetration and dissolution/precipitation mechanism.

If the corrosion mechanism has been well described, the kinetics of the reactions has still to be identified in order to couple it with impregnation.

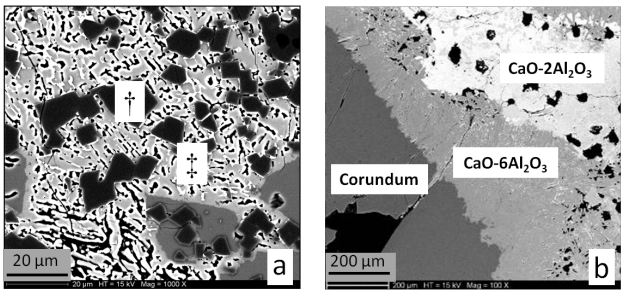

Fig. 1: Corrosion of alumina-magnesia in situ castables by secondary metallurgy slag. a): Micrograph of the matrix. † (Mg,Fe, Mn)O(Fe,Al_2)O_3 spinel. ‡ Impoverished slag CaO-Al_2O_3. b): Al_2O_3 aggregates and aluminates precipitation. According to Berjonneau et al. [1].

This communication presents a laboratory kinetic study of alumina refractories corrosion by alumina/lime/silica slag. Two different corrosion tests were performed on alumina grains with CaO-Al_2O_3 and CaO-Al_2O_3-SiO_2 slags. Ex situ corrosion tests were performed for long time to identify and quantify the precipitated phases and the time-resolved high-temperature X-ray diffraction analyses were performed during the in situ tests to determine the phase formation at the very beginning of the corrosion process.

MATERIALS AND EXPERIMENTS

Materials

Reaction kinetics tests were performed on pure ultra-fine alumina powder. Pure $CaCO_3$, Al_2O_3, and SiO_2 were used as raw materials to form two slags composed of the eutectic lime/alumina mixture (50 wt.%) for the binary slag (slag B) and of 45 wt.% CaO + 45 wt.% Al_2O_3 + 10 wt.% SiO_2 for the ternary slag (slag T). The oxides were mixed for 1 hr and the mixture was preheated at 1000 °C for 12 hrs to allow time for complete decomposition of $CaCO_3$. The treatment to form the slag was performed in a muffle high temperature furnace at 1650 °C for 1 hr. The platinum crucible containing the slag was then removed from the furnace and quenched with water. Quenching allowed releasing the slag from the crucible easier. X-ray diffraction (XRD) and differential scanning calorimetry analyses showed that both slags could contain $C_{12}A_7$ and C_3A. $C_{12}A_7$ is not expected in phase diagrams but exists under hydrated form because of air presence. In any event, slag was used in liquid state for the corrosion test.

Corrosion tests

Aluminates produced at equilibrium depend on the weight ratio. The results presented here were obtained from a first mixture of 85 wt.% of alumina with 15 wt.% of binary or ternary slag (mixtures B15 or T15) and a second one of 60 wt.% of alumina and 40 wt.% of the binary slag (mixture B40).

Two tests were performed:

- Corrosion tests with ex situ XRD analyses. The samples were quenched after the corrosion test and XRD analyses were performed at room temperature
- Corrosion tests with in situ analyses. Time-resolved high-temperature XRD analyses were performed during the tests.

The corrosion tests were carried out with temperature from 1500 up to 1600 °C.

CORROSION TESTS WITH EX SITU XRD ANALYSES

Ex situ test conditions

The corrosion tests were made in a muffle high temperature furnace at 1500 °C. When the temperature reached 1500 °C, the platinum crucible containing the mixture was put into the furnace for different periods of time from 10 min to 7 hrs. After each experiment, the sample was quenched from high temperature by immersion of the bottom of the crucible in water (fig. 2). The products were ground with ethanol and X-ray diffraction analyses were performed. Rietveld method was used to quantify the products.

Results for corrosion tests with ex situ XRD analyses

The expected equilibrium phases are alumina (11 wt.%) and hexa-aluminate of calcium (89 wt.%) for the mixture B15 at 1500 °C. It is worth noticing in figure 3 the presence of CA_2, which was not expected at equilibrium. After 7 h, the equilibrium state had not been reached yet. Another test performed in the same conditions with a dwell for 100 h showed roughly the same contents of the three phases indicating that corrosion process was quite stopped.

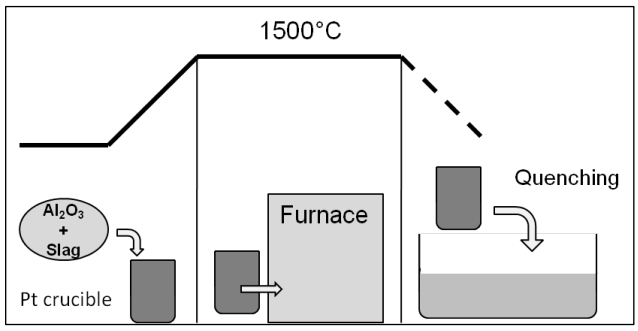

Fig. 2: Ex situ corrosion test on alumina powder.

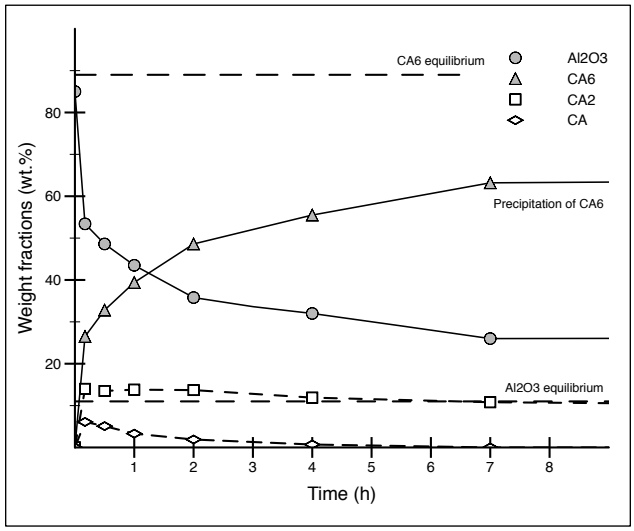

Fig. 3: Corrosion test. Mixture B15 – 1500 °C.

Figure 4 presents XRD quantification carried out for the mixture B40 at 1600 °C. The expected equilibrium phases are CA_6 (12 wt.%) and CA_2 (88 wt.%). This time, the crystallised phase CA was detected although it was not expected at equilibrium. After 7 h, the equilibrium state was not yet reached. Another test performed in the same conditions with a dwell for 24 h showed the equilibrium was reached; CA phase had disappeared. The alumina content changes barely from 2 hour while CA and CA_6 decrease in aid of CA_2. Scanning electron microscopy performed on corroded sample did not show vitreous phase.

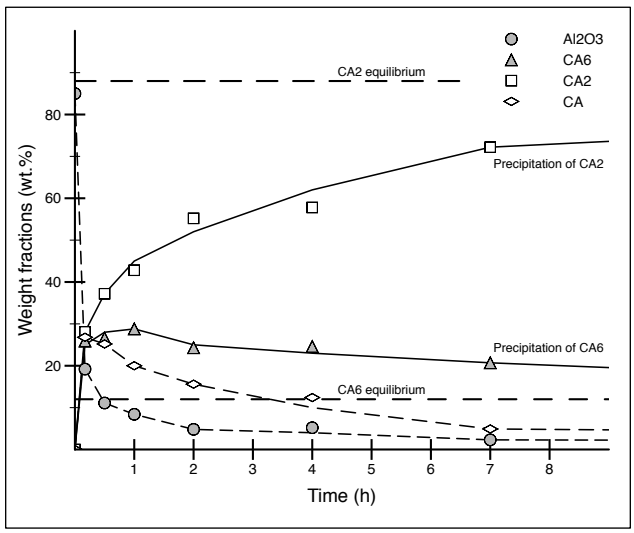

Fig. 4: Corrosion test. Mixture B40 – 1600 °C.

The corrosion tests can be divided into two stages involving two mechanisms (fig. 5):

1) In the early 10 min, the slag melts and reacts very quickly to form CA_6, CA_2, and CA layers. It can be observed that the CA_6 mass fraction (~20-25 wt.%) is almost the same for the both mixtures. The amount of dissolved alumina increases with the amount of slag but once CA_6 has formed, the remaining alumina does not react anymore. The slag was probably quite completely consumed after having formed CA_2 for the mixture B15 while it remains enough to dissolve CA_2 and to form CA for the mixture B40.
Once aluminate layers have precipitated, solid/solid reactions take place. While there is slag, Ca^{2+} and O_2^- ions from slag diffuse then through the layers and react at every interface Al_2O_3/CA_6, CA_6/CA_2 and CA_2/CA to dissolve the alumina richer layer and to increase the thickness of the crossed layer. The diffusion is however more and more limited with thickness increasing. In the same time, the slag dissolves the outer layer (CA_2 or CA, depending on the test) and leads to an indirect dissolution of the alumina grains [4].

2) When the slag is wholly consumed, the dissolution of the outer layer stops but solid diffusion reactions continue. For the mixture B15, calcium cations have to diffuse through the CA6 layer to react with alumina. The CA_6 layer thickness increases and the diffusion is lowered, stops even. For the mixture B40, cations coming from CA layer diffuse more easily through the CA_2 layer and react with CA_6 to form CA_2. CA_6 forms still a diffusion barrier but its thickness decreases and alumina dissolution continues to arise slowly till the disappearance of CA.

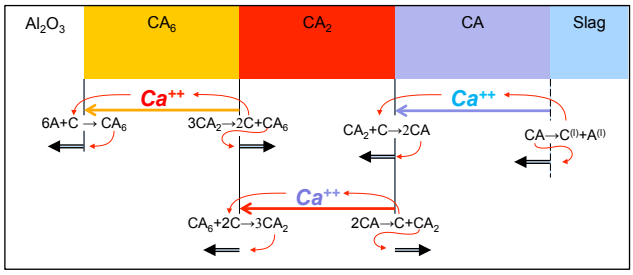

Fig. 5: Mechanism of indirect dissolution of alumina by alumina/lime/silica slag.

Moreover the results show that the dissolution/precipitation process arises very quickly, probably in less than 10 minutes. Addressing the dissolution kinetics led then to perform in situ XRD analyses.

CORROSION TESTS AND TIME-RESOLVED HIGH-TEMPERATURE X-RAY DIFFRACTION ANALYSES

In situ test conditions

A high-temperature strip heater chamber (HTK16 Anton Paar) was used for in situ XRD studies of phase formation. The corrosion tests were performed on an Equinox 3000 powder diffractometer (INEL brand), equipped with a CPS120, a copper source and a parabolic mirror [5-7]. The instrument was set in vertical mode. The asymmetric geometry (reflection) was necessary for such in-situ experiment. The angle of the incident X-ray beam was set at 15 ° with respect to the sample surface. The counting time was kept constant at 5 s per step.
The batch made of slag and alumina mixed powders was mixed with ethanol to form a paste that was applied directly and uniformly to the platinum heating-strip. The heat treatment consisted of three stages:

- Heating at 5 °C/s. Not compacting the batch and maximum temperature rate enabled to avoid reaction between the

refractory powder and the ground slag in solid state before the melting of the slag.
- Dwell for 15 minutes at 1600 °C
- Cooling at 5 °C/s.

In situ XRD analyses were performed during the three stages. The Rietveld analysis program Maud was used for the Rietveld refinement in this study [8,9].

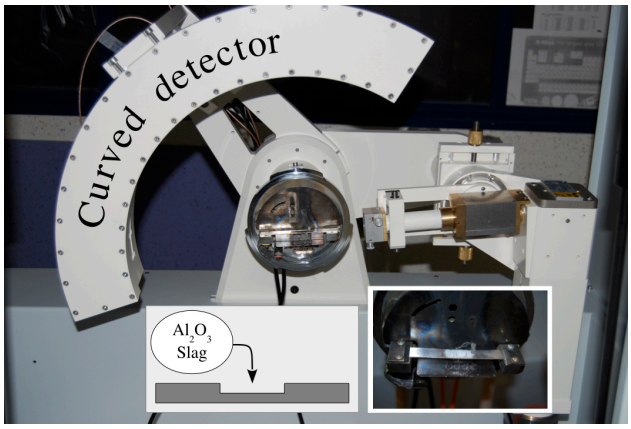

Fig. 5: In situ corrosion test with high-temperature XRD

Results for corrosion tests with in situ XRD analyses

Around 300 diffraction patterns were recorded during the corrosion test. The totality of the time series of the patterns is shown in Fig. 6 in the form of a 2D diagram. During the heating, the peaks corresponding to the alumina show good intensities and resolution and are in good agreement with ICCD data (PDF 01-070-5679) providing the thermal expansion of the lattice is taken into account. Due to the small amount of amorphous slag compared to the crystallised Al_2O_3, no broad peak is distinguishable from the background and alumina was the main phase observed. The slag was supposed to be amorphous owing to the quenching or could partially contain recrystallized aluminates as explained above. In any case, the rest of amorphous phase recrystallized at 900 °C to form $C_{12}A_7$ and C_3A in agreement with the results of differential scanning calorimetry and XRD analyses performed on the slag before use. Note that, apart from this recrystallization, no other phase crystallised confirming that no solid-state reaction occurred during the heating thanks the heating rate of 300 °C/min.

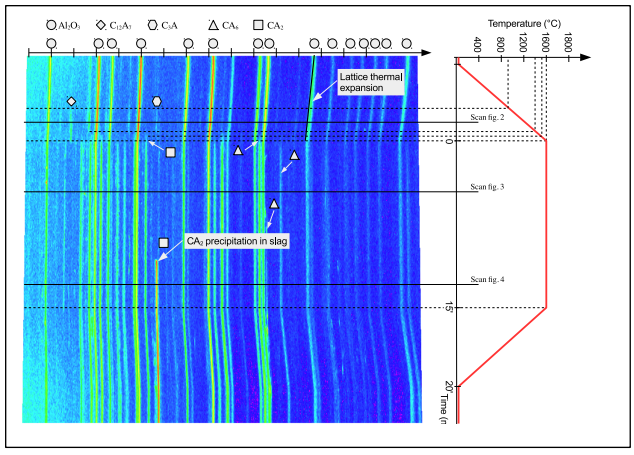

Fig. 6: 2D diagram of the XRD patterns recorded during the corrosion test. Abscise is 2θ angle from 15 to 100°. B15 – 1600 °C

The recrystallized phase started to disappear from 1390 °C. This value is slightly higher than the theoretical liquidus temperature (1360 °C) and the experimental one obtained with DSC (1370 °C). The difference may be explained by the temperature measurement uncertainties since the thermocouple is placed just below the platinum heating-strip and not right within the sample, but also by the increase of the temperature of 25 °C through the step taking 5 s. The $C_{12}A_7$ and C_3A phases had disappeared at 1600 °C while CA_6 and CA_2 started to precipitate from 1500 °C. As thought CA_2 peaks were observed from the beginning of the dissolution/precipitation, some peaks showed a sharp increase of their intensity while the other peaks of this phase continued to be more or less stable. Considering the SEM analyses of the corroded products, we deduced that CA_2 precipitated under two forms:

i) A monomineral layer forming a shell around the CA_6 layer, which formed itself a shell around the alumina grains;

ii) Grains of precipitated phase within the slag with specific structural orientation.

The mass fractions of the crystalline phases were quantified by Rietveld method. The liquid phase fraction and the corrected mass fraction of the crystalline phases were derived from the crystalline phase fractions by applying the mass balance according to the stoichiometric reactions and the thermodynamic equilibrium.

Figure 7 shows the XRD quantification carried out for mixture B15 for the corrosion test performed at 1600 °C. The expected equilibrium phases are Al_2O_3 (11 wt.%) and CA_6 (89 wt.%). The plot starts when the dwell temperature has been reached (1600 °C), i.e. after the heating stage. It can be observed that half of the alumina was dissolved after 5 minutes and its dissolution had stopped after 10 minutes, in agreement with ex situ results. CA_6, which is the main precipitating phase, increases with a similar rate. The slag amount decreased very quickly as well. For every quantification, the remaining slag is calculated by assuming its composition does not change (50 wt.% CaO + 50 wt.% Al_2O_3) although its actual alumina content increases up the solubility limit to form CA_2. It is therefore not sure that slag remained after 5 minutes (less than 5 wt.%). The amount of remaining slag might be added to the one of CA_2. This possible difference does not change the weight fraction of the stable phases Al_2O_3 and CA_6.

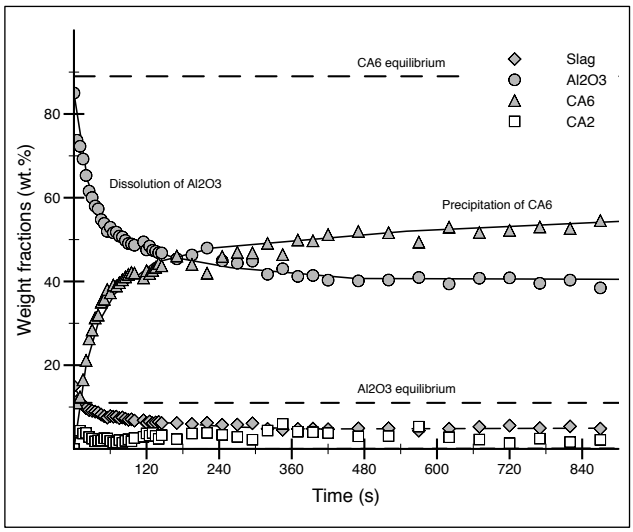

Fig. 7: Kinetics curves of in situ corrosion test. B15 – 1600 °C.

In situ corrosion test was performed with the mixture T15 to observe the effect of the silica (fig. 8). At 1600 °C, the expected phase at equilibrium are 6.6 wt.% slag + 62.3 wt.% CA_6 + 31.1 wt.% Al_2O_3. The corrosion rate is lower than that for binary mixture due to the higher viscosity of slag including silica. In addition to these stable phases, CA_2 precipitated like with the binary slag. Its weight fraction reached a maximum after 1 minute and decreased till the whole disappearance after 12 min,

when the equilibrium was quite reached. The maximum weight fraction of CA_2 corresponds to the stabilisation of the slag content. In a first stage, the slag provides the Ca^{2+} ions diffusing through the monomineral layers like with binary slag. Indirect dissolution by the slag takes place and yields the precipitation of the aluminates layers. When the slag has reached its solubility limit of alumina, this process stops while the solid diffusion continues. The corrosion process slows down as for the binary slag. CA_6 forms a chemical barrier but alumina has been less dissolved compared with the mixtures B15. Alumina aggregates are thus bigger and CA_6 layer is thinner even for a higher weight fraction. The cations Ca^{2+} can therefore diffuse through CA_6 layer and makes possible the thermodynamic equilibrium, which was not possible in the case of the mixture B15.

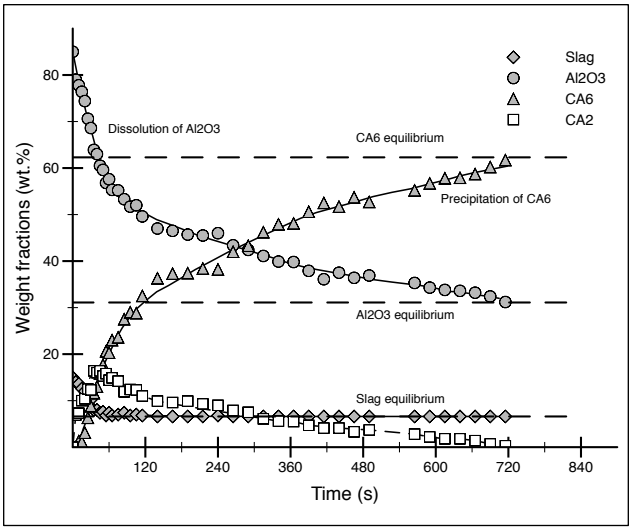

Fig. 8: Kinetics curves of in situ corrosion test. T15 – 1600 °C.

CONCLUSION

Ex situ X-ray diffraction analyses, i.e. performed at room temperature after quenching, showed that the corrosion of alumina aggregates by Al_2O_3-CaO-SiO_2 slag leads to the very fast precipitation of $CA_6/CA_2/CA$ layers and CA_6/CA_2 layers at 1500 °C and 1600 °C, respectively. For each temperature, the outer layer is not stable. In agreement with the thermodynamic calculations, it was observed that the corrosion results from an indirect dissolution process based on two mechanisms: a dissolution of the outer layer by the slag and a solid diffusion controlled reaction yielding, at each layers interface, the consumption of the inner layer and the growth of the outer one.

The in situ experiments, based on time-resolved high-temperature X-ray diffraction allowed for the study of the reactions during the very beginning of the corrosion. Using a high-temperature strip heater chamber made the slag to melt very quickly preventing solid-solid reaction between the slag and the alumina aggregates. A full 2θ pattern was recorded every 5 s by means of a Curved Position Sensitive detector (CPS120). It was then possible to quantify the precipitated phases by Rietveld method and the slag weight fraction was derived from mass balance. The results were in agreement with the ones from ex situ analyses. This technique also allowed to show the key role of the slag and to explain the difference of behaviour according to the slag composition and refractory/slag ratio.

REFERENCES

[1] Berjonneau J, Prigent P, Poirier J. The development of a thermodynamic model for Al_2O_3–MgO refractory castable corrosion by secondary metallurgy steel ladle slag. Ceramics International. 2009; 35 (2):623-635.

[2] Bale CW, Bélisle E, Chartrand P, Decterov SA, Eriksson G, Hack K, et al. FactSage thermochemical software and databases — recent developments. Calphad. 2009; 33 (2):295-311.

[3] Eriksson G, Pelton A. Critical evaluation and optimization of the thermodynamic properties and phase diagrams of the CaO-Al_2O_3, Al_2O_3-SiO_2, and CaO-Al_2O_3-SiO_2 systems. MTB. 1993; 24 (5):807-816.

[4] Lee WE and Zhang S. Direct and Indirect slag Corrosion of oxide and oxide – C Refractories. VII International Conference on Molten Slags Fluxes and Salts Proceedings. 2004; 309-319.

[5] Evain M, Deniard P, Jouanneaux A, Brec R. Potential of the INEL X-ray position-sensitive detector: a general study of the Debye–Scherrer setting. Journal of Applied Crystallography. 1993; 26(4):563-9.

[6] Scarlett NVY, Madsen IC, Manias C, Retallack D. On-line X-ray diffraction for quantitative phase analysis: Application in the Portland cement industry. Powder Diffraction. 2001; 16(02):71-80.

[7] Masson O, Guinebretiere R, Dauger A. Reflection Asymmetric Powder Diffraction with Flat-Plate Sample using a Curved Position-Sensitive Detector (INEL CPS 120). Journal of Applied Crystallography. 1996; 29(5):540-6.

[8] Lutterotti L, Bortolotti M. Object-oriented programming and fast computation techniques in Maud, a program for powder diffraction analysis written in Java. Compcomm Newsletter. 2003; 1:43-50.

[9] Le Bail A. Whole powder pattern decomposition methods and applications: A retrospection. Powder Diffraction. 2005; 20(04):316-326.